Active-Site Mutations of Diphtheria Toxin: Effects of Replacing Glutamic Acid-148 with Aspartic Acid, Glutamine, or Serine†

Brenda A. Wilson,‡ Karl A. Reich,‡,§ Beth R. Weinstein,‡,∥ and R. John Collier*,‡,⊥

Department of Microbiology and Molecular Genetics, Harvard Medical School, and Shipley Institute of Medicine, 200 Longwood Avenue, Boston, Massachusetts 02115

Received February 28, 1990; Revised Manuscript Received June 4, 1990

ABSTRACT: Glutamic acid-148, an active-site residue of diphtheria toxin identified by photoaffinity labeling with NAD, was replaced with aspartic acid, glutamine, or serine by directed mutagenesis of the F2 fragment of the toxin gene. Wild-type and mutant F2 proteins were synthesized in *Escherichia coli*, and the corresponding enzymic fragment A moieties (DTA) were derived, purified, and characterized. The Glu → Asp (E148D), Glu → Gln (E148Q), and Glu → Ser (E148S) mutations caused reductions in NAD:EF-2 ADP-ribosyltransferase activity of ca. 100-, 250-, and 300-fold, respectively, while causing only minimal changes in substrate affinity. The effects of the mutations on NAD-glycohydrolase activity were considerably different; only a 10-fold reduction in activity was observed for E148S, and the E148D and E148Q mutants actually exhibited a small but reproducible increase in NAD-glycohydrolytic activity. Photolabeling by nicotinamide-radiolabeled NAD was diminished ca. 8-fold in the E148D mutant and was undetectable in the other mutants. The results confirm that Glu-148 plays a crucial role in the ADP-ribosylation of EF-2 and imply an important function for the side-chain carboxyl group in catalysis. The carboxyl group is also important for photochemical labeling by NAD but not for NAD-glycohydrolase activity. The pH dependence of the catalytic parameters for the ADP-ribosyltransferase reaction revealed a group in DTA-wt that titrates with an apparent pK_a of 6.2–6.3 and is in the protonated state in the rate-determining step. As this titration is absent in the pH profiles of either of two mutants examined, DTA-E148Q or DTA-E148S, the apparent pK_a of 6.2–6.3 in the wild-type toxin may be due to an active-site imidazole, whose titration is affected by the presence or absence of the carboxyl group. Independent evidence indicates that there is a single histidine (His-21) within the active-site pocket of DTA, and we suggest that both His-21 and Glu-148 may be involved in the catalysis of ADP-ribosylation.

Many bacterial exotoxins act via enzymic reactions that involve covalent modification of target macromolecules within eucaryotic cells. For a major subset of such toxins, including diphtheria toxin (DT), *Pseudomonas aeruginosa* exotoxin A (ETA), cholera toxin, pertussis toxin, and others, the modification reaction involves transfer of the ADP-ribose portion of NAD to the respective target molecule (Jacobson & Jacobson, 1989; Collier & Mekalanos, 1980). Although the catalytic mechanism(s) and active sites of these toxins have not yet been described in detail, recent studies have yielded relevant information.

Diphtheria toxin has served as an important model system for studying ADP-ribosylating toxins (Collier & Mekalanos, 1980; Collier, 1982). DT is a 535-residue proenzyme that, after activation, catalyzes ADP-ribosylation of a posttranslationally modified histidine (diphthamide) on elongation factor 2 (EF-2). ADP-ribosylated EF-2 is inactive in mediating polypeptide chain elongation, and toxin-treated cells lose the ability to synthesize protein. This same mechanism is used by *P. aeruginosa* exotoxin A (ETA) to inhibit protein synthesis. DT, ETA, and many other ADP-ribosylating toxins also manifest weak NAD-glycohydrolase activity, detectable in the absence of the target protein, but the physiological significance of this activity is not yet known.

Activation of the native, proenzymic form of DT involves proteolytic "nicking" and reduction steps. Proteolysis of DT at a trypsin-sensitive site yields an amino-terminal A fragment (DTA; 193 residues) and a carboxy-terminal B fragment (DTB; 342 residues) linked by a disulfide bridge. Reduction of this disulfide then liberates the enzymically competent DTA from DTB. The B fragment binds the toxin to cell surface receptors and mediates entry of the A moiety into the cytoplasm.

Glutamic acid-148 was identified as a putative active-site residue in DTA by a unique photoaffinity labeling reaction. When complexes of DTA with NAD are irradiated at 254 nm, Glu-148 is specifically and efficiently photolabeled (Carroll & Collier, 1984; Collier, 1986; Carroll et al., 1985a,b). The photoproduct formed at position 148 has been shown to contain the entire nicotinamide moiety of NAD covalently linked, through C_6, to the decarboxylated γ-methylene carbon of the glutamic acid residue (Carroll et al., 1985a,b). Functionally similar and presumably homologous residues in ETA (Glu-553) (Carroll & Collier, 1987) and pertussis toxin (Glu-129) (Barbieri et al., 1989) have been identified by the same photolabeling reaction. Additionally, X-ray crystallographic structure analysis of native ETA indicated that Glu-553 is indeed located within the active-site cleft of the catalytic domain III (Allured et al., 1986; Collier, 1989).

In both DT and ETA, the putative active-site glutamic acid residues have been subjected to site-directed mutagenesis. The conservative substitution of aspartic acid for Glu-148 in DT or Glu-553 in ETA caused drastic (≥100-fold) reduction in

† The work was supported by USPHS Grants AI22021 and AI22848 from the National Institute of Allergy and Infectious Diseases.

* Corresponding author.

‡ Harvard Medical School.

§ Present address: Department of Biotechnology, Institut Pasteur, 25 Rue du Dr. Roux, 75724 Paris Cedex 15, France.

∥ Present address: Division of Infectious Diseases, Mount Auburn Hospital, 330 Mount Auburn Street, Cambridge, MA 02238.

⊥ Shipley Institute of Medicine.

0006-2960/90/0429-8643$02.50/0

NAD:EF-2 ADP-ribosyltransferase activity (Tweten et al., 1985; Douglas & Collier, 1987; Carroll & Collier, 1987), and other substitutions (Lukac & Collier, 1988) or deletion of the Glu-553 residue (Lukac et al., 1988) caused even greater effects. These results support the notion that these glutamic acid residues are crucial for catalysis. Here we report the results of studies in which Glu-148 was mutated to aspartic acid, glutamine, or serine and the effects on NAD:EF-2 ADP-ribosyltransferase, NAD-glycohydrolase, and photoaffinity labeling activities of DTA were characterized.

Experimental Procedures

Mutagenesis. The *Eco*RI–*Hin*dIII fragment encoding the DT gene fragment F2 (Tweten & Collier, 1983) was subcloned into M13mp19. A 22-base oligonucleotide (5′ dAGGGGATCCGTTATGAGCAGAA 3′) containing two base changes (underlined) was used to create a *Bam*HI restriction site (GGATCC) by replacing an A with a C and to change the GTG start codon in the wild-type F2 gene to an ATG start codon. This mutagenized gene was subsequently used as the parent clone for all further manipulations of the DT sequence. This was subsequently cloned into the *Bam*HI–*Hin*dIII sites of pCDtac2 (Douglas et al., 1987) and renamed ptacF2. The synthetic oligonucleotide (5′ dCGTTGATTATATT 3′) (change underlined) was used to mutate the GAA codon at amino acid position 148 to GAT, thereby converting glutamic acid at this position to aspartic acid. A second synthetic oligonucleotide (5′ dCGTTCAATATATT 3′) was used to change the GAA codon at amino acid position 148 to CAA, thereby converting glutamic acid at this position to glutamine. Finally, a third synthetic oligonucleotide (5′ dCTAGCGTTTCCTATATTAA 3′) containing a three-base substitution (underlined) was used to change the GAA codon (glutamic acid) at position 148 to TCC (serine).

Oligonucleotide-directed in vitro mutagenesis was performed with a commercially available kit (Amersham) according to the manufacturer's instructions (Zoller & Smith, 1983; Taylor et al., 1985a,b). M13 bacteriophage supernatants were screened as previously described (Douglas & Collier, 1987; Maniatis et al., 1982). Positive clones were plaque purified and the mutations were verified by dideoxy sequencing using Sequenase (United States Biochemicals) according to manufacturer's instructions (Sanger et al., 1977). The 1232-bp *Bam*HI–*Hin*dIII fragment from sequenced clones was isolated from M13 RF DNA and inserted into *Bam*HI–*Hin*dIII-digested, gel-purified pCDtac2 vector. The new plasmids were transformed into *Escherichia coli* strain JM103 (Douglas et al., 1987; Leong et al., 1983a,b) and renamed ptacF2-E148D, ptacF2-E148S, and ptacF2-E148Q. All clones used in this study were colony purified and either recloned into M13mp19 and resequenced or double-stranded dideoxy sequenced (Sanger et al., 1977) directly to confirm that the desired mutation was present in the gene used to express the recombinant protein.

Growth and Harvesting of Cells. A Microferm fermenter (New Brunswick Scientific) was used to grow the mutant clones. Aerated L-broth (10 L), prewarmed to 37 °C and containing 100 μg of ampicillin/mL, was inoculated with 150 mL of an overnight culture of the appropriate mutant, grown under selection conditions. The cultures were oxygenated at 8 L/min and stirred at 550 rpm. The cultures were induced at an OD_{580} = 0.16 with 1 mM isopropyl β-D-thiogalactopyranoside (Sigma) (de Boer et al., 1983), and growth was continued until OD_{580} = 2.0. Cells were harvested by using a Pellicon Tangential Flow Filtration System (Millipore) fitted with a 0.45-μm filter and concentrated to approximately 1 L. The resulting cell suspension was washed with 5 L of ice-cold 100 mM Tris-HCl buffer, pH 8.0, dispensed into prechilled GS-3 (Sorvall) centrifuge tubes, and centrifuged at 6000*g* for 20 min. The cells were resuspended in 350 mL of cold 100 mM Tris-HCl buffer, pH 8.0, containing 20% sucrose.

Periplasmic Extraction. The resuspended cells were extracted with lysozyme and EDTA (Fischetti et al., 1986) by mixing on ice with an equal volume of freshly prepared 100 mM Tris-HCl buffer, pH 8.0, containing 20% sucrose, 10 mM EDTA, and 0.5 mg of lysozyme/mL (egg white, Calbiochem). After 15–20 min, the spheroplasts were stabilized by addition of $MgCl_2$ to a final concentration of 50 mM. The cells were then centrifuged for 30 min at 11000*g* in a Sorvall RC5-B centrifuge.

Ammonium Sulfate Precipitation. The periplasmic extract was precipitated in the cold by slow addition of solid ammonium sulfate (Ultrapure, Schwarz/Mann) to 75% saturation (47.6 g/100 mL). The suspension was stirred overnight, and the protein pellet was collected by centrifugation at 11000*g* for 30 min. After the pellet was resuspended in 50 mM Tris-HCl buffer, pH 8.2, containing 1 mM EDTA (TE), the conductivity of the resulting solution was measured to give an estimate of the $(NH_4)_2SO_4$ concentration. Solid $(NH_4)_2SO_4$ was added to the solution to bring the concentration to the same conductivity as 1 M $(NH_4)_2SO_4$ in TE. This and subsequent steps were performed at room temperature.

Phenyl-Sepharose Chromatography. The protein-containing solution was applied to a phenyl-Sepharose (Pharmacia) column (12 mL of resin/100 mg of total protein) preequilibrated with 1 M $(NH_4)_2SO_4$ in TE. The column was eluted with a linear gradient of 1–0 M $(NH_4)_2SO_4$ in TE. Column fractions (2 mL) were assayed for protein content by measuring absorbance at 280 nm and for ionic strength by monitoring conductivity. To locate immunoreactive material in the column eluate, aliquots of column fractions (10 μL) were applied to nitrocellulose membrane filter sheets (presoaked in 25 mM Tris-HCl buffer, pH 8.3, containing 192 mM glycine and 0.1% SDS) sandwiched in a slot blotter (Schleicher and Schuell). The filters were dried in situ with a water aspirator for 30 s and then immersed and shaken in blocking buffer (10 mM Tris-HCl buffer, pH 8.0, containing 2 mM EDTA, 50 mM NaCl, and 1% hemoglobin). The nitrocellulose sheets were then probed for immunoreactive material with ^{125}I-labeled, affinity-purified horse anti-DT antibody (Tweten et al., 1985).

Partial Proteolysis of F-2 Proteins. Analytical digestions were performed on the combined and concentrated phenyl-Sepharose fractions to determine the conditions required for optimum cleavage of F2-E148D, F2-E148S, and F2-E148Q to their respective A fragments. Limited proteolysis was performed at 25 °C in the presence of 1 mM NAD (free acid, Boehringer Mannheim) with TPCK-treated trypsin (Sigma). Protease concentrations in the range 0.063–0.6% were employed, and the course of the digestion was monitored as a function of time. Reactions were terminated by the addition of soybean trypsin inhibitor (Sigma) to a final concentration of 1% and analyzed by Western blots of reducing and nonreducing SDS–polyacrylamide gels. The conditions found to give optimum cleavage of the F2 proteins were as follows: F2-E148D, 0.125% trypsin for 90 min; F2-E148Q and F2-E148S, 0.125% trypsin for 60 min. Preparative digestions were subsequently performed under appropriately scaled conditions.

Selective Elution of DTA. The resulting "nicked" F2 protein solutions were brought to 1 M $(NH_4)_2SO_4$ and reap-

plied to a column of phenyl-Sepharose (10 mL of resin/100 mg of total protein), preequilibrated with 1 M $(NH_4)_2SO_4$ in TE. A linear gradient from 1 M to 0.5 M $(NH_4)_2SO_4$ in TE was passed through the column before the fragment A moieties were specifically eluted with a step gradient of 0.47 M $(NH_4)_2SO_4$ in TE, containing 40 mM DTT. The elution of DTA was monitored by Coomassie stains of SDS–polyacrylamide gels. The fractions containing DTA were combined, concentrated by using Centricon concentrators (Amicon), and washed three times with TE containing 5 mM DTT.

Final Purification of DTA. The phenyl-Sepharose-purified toxin samples were further purified by treating the solutions (~1 mg/mL total protein concentration) in the presence of 1–2 mM NAD at 50 °C for 15–20 min, followed by centrifugation at 16000*g* for 10 min to remove precipitated protein. The supernatants were then purified to >99% homogeneity by anion-exchange chromatography using a Mono-Q HR 5/5 FPLC column (Pharmacia, 5 × 50 mm) with a linear gradient of 0–300 mM KCl in 20 mM Tris-HCl buffer, pH 7.5, containing 10 mM β-mercaptoethanol and 0.2 mM EDTA.

NAD:EF-2 ADP-Ribosyltransferase Assay. Initial rates of ADP-ribosylation of EF-2 by toxin were monitored by the incorporation of the radiolabeled ADP-ribose moiety of NAD into the TCA-precipitable protein fraction of the reaction mixture. [*Adenine*-2,8-$^3H_2$]NAD (32.8 Ci/mmol, NEN) was diluted to a final specific activity of 1.2 Ci/mmol with unlabeled NAD (Boehringer Mannheim) to give a final concentration of 208 μM. The final concentrations of toxin used in the reactions were 5.0 nM for DTA-wt, 0.6 μM for DTA-E148D, 0.5 μM for DTA-E148Q, and 1.4 μM for DTA-E148S. Reactions in a final volume of 50 μL of 50 mM Tris-HCl buffer, pH 8.0, containing 1 mM EDTA, 10 mM DTT, 50 μg of BSA/mL, and the specified concentrations of NAD and EF-2 for the kinetic experiments (see below) were incubated with the DTA samples at 25 °C for 3.0 min. Aliquots (45 μL) were removed, applied to 3MM (Whatman) paper saturated with trichloroacetic acid (TCA), and then washed twice with 5% TCA, dried in methanol, and counted with 3 mL of ACS fluor (Amersham) in an 1209 Rackbeta scintillation counter (LKB). The specificity of incorporation of radiolabel from NAD into EF-2 by the wild-type and mutant toxins was confirmed by allowing the reaction to go to completion, removing aliquots from the reaction mixture, and separating the protein components by SDS–polyacrylamide gel electrophoresis. The proteins were then electrophoretically transferred from the gel to a nitrocellulose membrane filter, and the bands corresponding to radiolabeled product were analyzed by autoradiography. From the intensities of the bands (data not shown), it was determined that greater than 99% of the acid-precipitable radioactivity was attributed to ADP-ribosylated EF-2.

NAD-Glycohydrolase Assay. Initial rates of NAD-glycohydrolysis by toxin were determined by the release of free radiolabeled nicotinamide into solution, resulting from the hydrolysis of [*nicotinamide*-4-^{3}H]NAD (3.0 Ci/mmol, 333 μM, Amersham). The assays were performed at varying NAD concentrations in the presence of toxin at 25.0 °C for 4–6 h in a final volume of 50 μL of 50 mM Tris-HCl buffer, pH 8.2, containing 1 mM EDTA, 5 mM DTT, and 50 μg of BSA/mL. The final concentrations of toxin used in the reactions were 0.6 μM for DTA-wt, 0.3 μM for DTA-E148D, 0.5 μM for DTA-E148Q, and 6.0 μM for DTA-E148S. The reactions were terminated by addition of 30 μL of 0.5 M sodium borate buffer, pH 8.0, and extracted with 200 μL of water-saturated ethyl acetate. Aliquots (160 μL) of the organic phase were removed and counted in 3 mL of ACS fluor (Amersham). The data corrected by substraction of the radioactivity due to nonenzymatic hydrolysis of NAD.

Table I: Kinetics of ADP-Ribosyltransferase Activity[a]

	DTA-wt	DTA-E148D	DTA-E148Q	DTA-E148S
(a) Fixed [EF-2], Variable [NAD]				
K_m (μM) (NAD)	9.0	11.2	12.2	8.8
k_{cat} (min^{-1})	58.8	0.60	0.32	0.19
rel k_{cat}	1	0.010 (1/98)	0.0054 (1/184)	0.0032 (1/309)
k_{cat}/K_m (M^{-1} min^{-1})	6.5×10^6	5.4×10^4	2.6×10^4	2.1×10^4
rel k_{cat}/K_m	1	0.0083 (1/121)	0.0040 (1/251)	0.0032 (1/311)
(b) Fixed [NAD], Variable [EF-2]				
K_m (μM) (EF-2)	0.9	1.6	1.5	1.7
k_{cat} (min^{-1})	77.7	1.7	0.60	0.49
rel k_{cat}	1	0.022 (1/46)	0.0078 (1/129)	0.0063 (1/159)
k_{cat}/K_m (M^{-1} min^{-1})	85×10^6	1.0×10^6	4.1×10^5	3.0×10^5
rel k_{cat}/K_m	1	0.012 (1/85)	0.0049 (1/205)	0.0035 (1/283)

[a] The experimental data were all determined to be statistically accurate to a standard deviation of not greater than ±10%.

Table II: Kinetics of NAD-Glycohydrolase Activity[a]

	DTA-wt	DTA-E148D	DTA-E148Q	DTA-E148S
K_m (μM) (NAD)	11.0	9.2	9.5	11.5
k_{cat} (min^{-1})	27×10^{-3}	37×10^{-3}	45×10^{-3}	2.3×10^{-3}
rel k_{cat}	1	1.4	1.7	0.085
k_{cat}/K_m (M^{-1} min^{-1})	2500	4000	4800	200
rel k_{cat}/K_m	1	1.6	1.9	0.080
K_d (μM) (NAD)	9.3	8.7	12.7	12.6

[a] The experimental data were all determined to be statistically accurate to a standard deviation of not greater than ±10%.

Kinetics Experiments. Initial rate data for the single-substrate NAD-glycohydrolase reaction were collected under conditions where NAD concentrations were varied from $0.2K_m$ to $2.5K_m$. Initial rate data for the ADP-ribosyltransferase reaction were similarly determined for NAD binding at fixed EF-2 concentrations (2.5 μM) and varying NAD concentrations from $0.2K_m$ to $2.5K_m$ and for EF-2 binding at fixed NAD concentrations (20.8 μM) and varying EF-2 concentrations from $0.2K_m$ to $2.5K_m$. The kinetic parameters were obtained by analysis of Lineweaver–Burk or Eadie–Hofstee plots of initial velocities for ADP-ribosylation reaction from at least three separate experiments, each performed in duplicate, and are summarized in Tables I and II.

Fluorescence Quenching. The decrease in intrinsic fluorescence of DTA as a function of NAD concentration was measured at 25.0 °C. Solutions of protein (1.5 mL, 500 nM) were excited at 285 nm (1 nm band-pass) and the fluorescence intensity was measured at 335 nm (10 nm band-pass) in an SPF 500C spectrofluorometer (Aminco) in the ratio mode. The fluorescence decrease of L-tryptophan as a function of NAD concentration was used to correct for NAD self-quenching.

Photolabeling. The kinetics of photoaffinity labeling were monitored by the incorporation of radioactivity from [*carbonyl*-^{14}C] NAD (1.63 GBq/mmol, Amersham) into the TCA-precipitable protein fraction of the reaction mixture. Solutions (70 μL) containing 7.5 μM protein and 50 μM NAD were irradiated (254 nm) at 0 °C with a germicidal lamp (GE, 2.5 mW/cm^2). At the indicated intervals, aliquots were re-

moved, applied onto TCA-saturated 3MM (Whatman) paper, and then washed twice in 5% TCA, dried in methanol, and counted in 3 mL of ACS fluor (Amersham).

Results

Mutagenesis and Expression. Mutagenesis was performed on the F2 gene fragment of DT, which is bounded by two *Msp* restriction sites (Tweten & Collier, 1983), and the gene fragment was expressed in *E. coli* JM103. The F2 protein contains all of the A fragment (residues 1–193) and approximately 60% of the B fragment but lacks the carboxy-terminal receptor-binding domain of whole toxin required for cytotoxicity. The F2 protein can be cleaved and reduced in a manner analogous to that employed in the activation of whole DT to yield enzymically active fragment A (DTA) and the truncated F2-B fragment. The F2 gene fragment can be manipulated and expressed under BL1 + EK1 containment conditions, in compliance with NIH guidelines regulating the heterologous expression of diphtheria toxin related proteins.

Oligonucleotide-directed mutagenesis was used to construct the mutants F2-E148D, F2-E148Q, and F2-E148S. The procedure involved a strand selection step that generates predominantly homoduplex mutant DNA (Zoller & Smith, 1983; Taylor et al., 1985a,b). DNA sequence analysis confirmed the presence of the desired base changes in each of the expression vectors, ptacF2-E148D, ptacF2-E148Q, and ptacF2-E148S, and confirmed that no second-site mutations had occurred within the mutagenized fragment. We introduced a *Bam*HI site at position 96 in the F2 gene in order to clone the gene into the corresponding site of pCDtac2 (Douglas et al., 1987). Protein expression was enhanced by changing the wild-type GTG initiation codon to ATG. Each of the F2 mutant proteins was expressed in *E. coli* under the control of the isopropyl β-D-thiogalactopyranoside (IPTG) inducible *tac* promoter (de Boer et al. 1983).

Purification of Mutant and Wild-Type Proteins. Since the F2 protein possesses a leader sequence that promotes secretion of the protein into the periplasmic space of *E. coli*, where it is then processed to the mature form (Douglas et al., 1987), we isolated the mutant F2 proteins from periplasmic extracts. We additionally isolated the wild-type F2 protein from *E. coli* extracts as a control. The purification scheme, developed from a knowledge of the hydrophobic properties of the B moiety of F2 protein and characteristics of the linkage between the A and B moieties, was a three-step procedure.

In the first step, the periplasmic extract was concentrated by precipitation with ammonium sulfate and fractionated by hydrophobic interaction chromatography to separate intact F2 protein from proteolytic fragments. The second step involved treating the partially purified F2 protein with trypsin to cleave the polypeptide at the A–B junction. The resulting "nicked" F2 protein consisted of fragment A disulfide-linked to the hydrophobic F2-B fragment. In the final step, the nicked molecule was adsorbed to a second hydrophobic column, primarily through interactions of the F2-B moiety, and fragment A was specifically released by reduction of the disulfide bridge linking it to F2-B fragment.

Step 1. The concentrated periplasmic extract in 1 M $(NH_4)_2SO_4$ was applied to a phenyl-Sepharose column and eluted with a reverse salt gradient. Three peaks of cross-reacting material were identified by immunoblotting. The first peak corresponded to free fragment A; the second, to a proteolytic fragment of F2 (estimated 32000 daltons); and the third, to the full-length F2 protein.

Step 2. Conversion of the partially purified F2 protein from the intact to the "nicked" form was accomplished by incubating material from the third peak of cross-reacting material from step 1 with trypsin in the presence of 1–2 mM NAD, which protects the fragment A moiety from proteolytic attack. Soybean trypsin inhibitor was added to terminate proteolysis, and the sample was brought to 1 M $(NH_4)_2SO_4$.

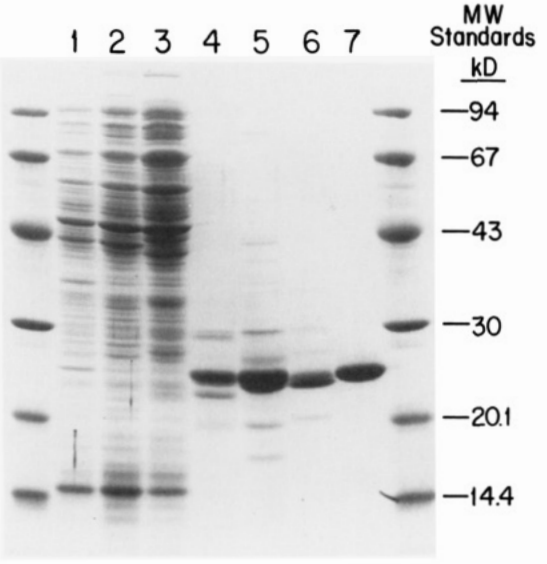

FIGURE 1: SDS–polyacrylamide gel electrophoretic analysis of samples from different stages of DTA purification. Lane 1, Periplasmic extract after ammonium sulfate precipitation and dialysis; lane 2, after the first phenyl-Sepharose column; lane 3, after partial proteolysis with trypsin; lane 4, DTA-E148D after second phenyl-Sepharose column; lane 5, DTA-E148S; lane 6, DTA-E148Q; lane 7, DTA-wt.

Step 3. The sample from step 2 was then applied to a second phenyl-Sepharose column, preequilibrated in 1 M $(NH_4)_2SO_4$, and the concentration of $(NH_4)_2SO_4$ was reduced to 0.5 M with a linear gradient. At ammonium sulfate concentrations below 0.5 M, free fragment A, unlike F2 protein and F2-B fragment, does not bind to the resin and could be specifically released from the column after reduction of the disulfide linkage with 40 mM dithiothreitol.

This protocol was used to purify all three mutant forms of fragment A (DTA-E148D, DTA-E148S, and DTA-E148Q), as well as the wild-type A fragment. The products were at least 90% pure, as judged by densitometry of Coomassie-stained SDS–polyacrylamide gels. Figure 1 shows the band patterns of the periplasmic extract (lane 1), the phenyl-Sepharose pool before (lane 2) and after (lane 3) partial proteolysis, and the eluted A fragments from the second phenyl-Sepharose column (DTA-wt, DTA-E148D, DTA-E148S, and DTA-E148Q, lanes 4, 5, 6, and 7, respectively). Greater purity (>99%) was attained, when desired, by treating the protein solution in the presence of 1–2 mM NAD at 50 °C for 15–20 min, followed by centrifugation to remove precipitated protein. Under these conditions DTA is quite stable, whereas F2, F2-B fragment, and other remaining contaminating proteins are denatured and precipitate. This procedure may then be followed by FPLC purification using a Mono-Q anion-exchange column, with a linear elution gradient of 0–300 mM KCl in 20 mM Tris-HCl buffer, pH 7.6, containing 10 mM β-mercaptoethanol and 0.2 mM EDTA. The final yield of purified toxin was usually 4–5 mg of DTA/10 L of starting cell culture, with the overall yield of purified toxin estimated to be ~50% from the crude periplasmic extracts.

Photoaffinity Labeling. The kinetics of photoaffinity labeling of the mutant DTA fragments by [*carbonyl*-^{14}C] NAD are shown in Figure 2. Under the described conditions, the E148D mutant was photolabeled at a rate equivalent to about 12% that of the wild-type DTA, whereas the E148Q and

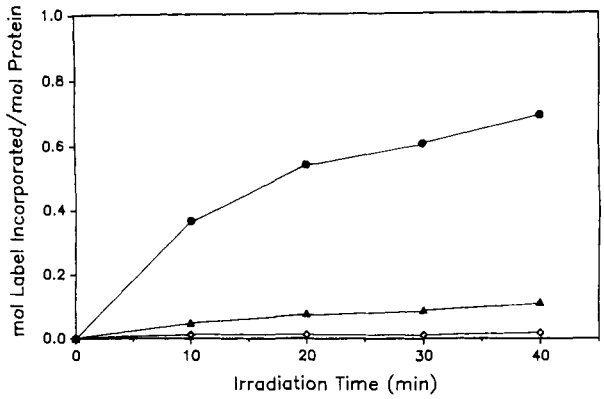

FIGURE 2: UV-induced labeling of DTA-wt (●), DTA-E148D (▲), DTA-E148Q (◇), DTA-E148S (◇), and ovalbumin (◇) in the presence of [*carbonyl*-^{14}C]NAD. Reaction mixtures containing 50 mM Tris-HCl buffer, pH 7.5, DTA (7.5 μM), and radiolabeled NAD (50 μM) were irradiated at 254 nm. At the times indicated, aliquots (45 μL) were removed and applied to TCA-saturated 3MM (Whatman) paper. After several washes in 5% TCA, the acid-precipitable radioactivity was determined.

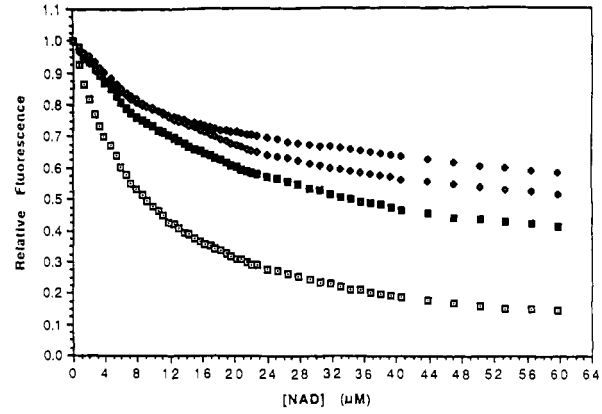

FIGURE 3: Quenching of intrinsic protein fluorescence by NAD for DTA-wt (□), DTA-E148D (◆), DTA-E148Q (■), and DTA-E148S (◇). Assays were performed as described under Experimental Procedures. Data were corrected for NAD self-quenching, and the percent quenching at each NAD concentration was calculated from the data and analyzed by Scatchard plots to determine the dissociation constants for the wild-type and mutant proteins. The K_d values obtained are summarized in Table II.

E148S mutants gave no detectable levels of labeling (<1% that of the wild-type toxin).

Kinetic Studies. An evaluation of the effect of replacement of Glu-148 with aspartate, glutamine, or serine on the overall conformation of the DTA molecule was provided by determining the binding affinities for the substrates NAD and EF-2. The K_m values for NAD binding to the mutant and wild-type toxins at pH 8.0 and 25 °C were obtained from kinetic analyses of the NAD:EF-2 ADP-ribosyltransferase and NAD-glycohydrolase activities.

For the single-substrate NAD-glycohydrolase reaction, initial rate data were collected under conditions where NAD concentrations were varied from $0.2K_m$ to $2.5K_m$, and the kinetic parameters, obtained by analysis of the results, are summarized in Table II. Whether determined from Eadie–Hofstee or Lineweaver–Burk plots, the K_m values of 9.2, 9.5, and 11.5 μM obtained for NAD binding to the E148D, E148Q, and E148S mutants, respectively, were close to that of the wild-type toxin (11.0 μM). The K_m values for NAD binding to toxin for the ADP-ribosyltransferase reaction were similarly determined from initial rate data obtained at fixed EF-2 concentrations (2.5 μM) and varying NAD concentrations from $0.2K_m$ to $2.5K_m$. The kinetic parameters, obtained by analysis of the results, are summarized in Table Ia. The K_m values of 9.0, 11.2, 12.2, and 8.8 μM for NAD binding to wt, E148D, E148Q, and E148S toxins were in agreement with those determined for the single-substrate reaction and indicated that, within experimental error, none of the mutants showed altered affinity for NAD.

Additionally, dissociation constants for NAD binding to the mutant and wild-type toxins at pH 8.0 and 25 °C were measured independently of enzymatic activity by monitoring the decrease in intrinsic protein fluorescence at 335 nm (excitation at 285 nm) as a function of NAD concentration (Figure 3) and subjecting the data to Scatchard analysis after correction for the inner filter effect. The K_d value obtained for NAD binding to the wild-type DTA, 9.3 μM, was in agreement with values published earlier (Kandel et al., 1974; Chung & Collier, 1977; Collier et al., 1974). The K_d values for NAD binding to the mutants E148D, E148Q, and E148S of 8.7, 12.7, and 12.6 μM, respectively, were close to that of the wild-type DTA and are consistent with the K_m values obtained for the ADP-ribosylation and NAD hydrolysis reactions. The differences in the extent of fluorescence quenching observed between the wild-type and mutant toxins were reproducible and may reflect minor perturbation in protein conformation upon ligand binding due to small changes in steric or electronic interactions between the tryptophans and the NAD substrate or other active-site residues.

No major change in the binding affinity for EF-2 was observed for any of the mutants in analogous initial rate experiments, where NAD concentration was fixed (20.8 μM) and EF-2 concentrations were varied from $0.2K_m$ to $2.5K_m$. The kinetic parameters, obtained by analysis of the Lineweaver–Burk or Eadie–Hofstee plots of initial velocities for the ADP-ribosylation reaction, are summarized in Table Ib. The K_m values of 1.6, 1.5, and 1.7 μM for EF-2 binding to the E148D, E148Q, and E148S mutants, respectively, were only slightly higher than that of the wild-type toxin (0.9 μM). Thus, substitution of aspartate, glutamine, or serine for glutamate at position 148 apparently causes little or no perturbation of the overall protein conformation as evidenced by the lack of any significant effect on both K_m and K_d for NAD or on K_m for EF-2.

The kinetic parameters K_m, k_{cat}, and k_{cat}/K_m for both the mutant and wild-type toxins at 25 °C in 50 mM Tris-HCl buffer, pH 8.0, are summarized in Table I for the NAD:EF-2 ADP-ribosyltransferase reaction and in Table II for the considerably slower glycohydrolysis of NAD. Whereas the K_m values for NAD and EF-2 binding to the DTA mutants were essentially unchanged, a >100-fold decrease in both k_{cat} and k_{cat}/K_m was found for each of the Glu-148 mutants as compared with the wild-type toxin under the described conditions. Even the conservative aspartate mutation resulted in an enzyme that was considerably slower (100-fold lower k_{cat}) and less efficient (120-fold lower k_{cat}/K_m) than the wild-type toxin. The glutamine and serine mutations showed even greater effects on k_{cat} and k_{cat}/K_m (180- and 250-fold lower for E148Q and 310- and 310-fold lower for E148S, respectively). In each case, the kinetic effects were almost exclusively on k_{cat} and not on K_m.

On the other hand, the substitutions at position 148 affected NAD-glycohydrolase activity to a much lesser extent than ADP-ribosyltransferase activity. Indeed, the mutants even exhibited a different order of relative activity in the hydrolysis reaction. The E148D and E148Q mutants actually displayed slightly higher k_{cat}'s (1.4- and 1.7-fold higher, respectively) and catalytic efficiencies (1.6- and 1.9-fold higher, respectively) than the wild-type toxin, and the k_{cat} and k_{cat}/K_m for the

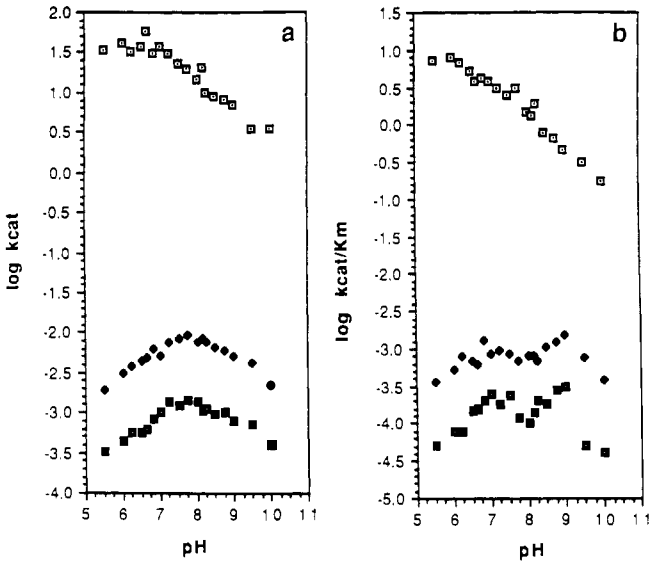

FIGURE 4: pH profiles of (a) log k_{cat} and (b) log $k_{cat}/K_{m[NAD]}$ for ADP-ribosylation of EF-2 by DTA-wt (□), DTA-E148Q (◆), and DTA-E148S (■). The kinetic data were obtained at varying pH values as described in the text.

E148S mutant were only about 10-fold lower than those for wild-type DTA. Again, since there were no significant changes in the K_m for NAD binding to the mutants compared to the wild-type toxin, the differences in the activities for the mutant enzymes were attributed to the differences in k_{cat}.

pH Profile Studies. Apparent kinetic parameters of ADP-ribosylation for DTA-wt, DTA-E148Q, and DTA-E148S were next determined over the pH range 5.5–10.0. The stability of the toxins was first determined at each pH by preincubation of the toxins for the normal assay time at these pH values before addition of substrates (data not shown). Although there was slight denaturation/inactivation (5%) of the proteins at pH values 9.5, inactivation at all other pH values was negligible over the time scale used. The stability of EF-2 was likewise examined by testing for its ability to be ADP-ribosylated after preincubation for the normal assay time at the various pH values (data not shown). Results showed it to be stable over the pH range 6.0–9.5, with no more than 10% loss of ADP-ribose acceptor activity occurring at the pH values of 5.5 and 10.0. NAD was found to be stable for the duration of the assay over the pH range 5.5–9.0, with less than 5% decomposition occurring above pH 9.0. Additionally, the K_m values for NAD were not found to vary by more than 2-fold throughout the pH range tested, nor was there any significant change in the extent of quenching of intrinsic protein fluorescence by NAD at these pH values (data not shown). Thus, the kinetic parameters needed only to be slightly corrected for inactivation at the extreme pH values.

As shown in Figure 4, the pH dependence curves of the observed k_{cat} and $k_{cat}/K_{m(NAD)}$ values for DTA-wt differed dramatically from those of the two active-site mutants that were examined, DTA-E148Q and DTA-E148S. It is apparent that DTA-wt has an ionizable group that is not evident in the two mutants tested. By plotting $(k_{cat})^{obsd}$ vs $(k_{cat})^{obsd}/[H^+]$ and $(k_{cat}/K_m)^{obsd}$ vs $(k_{cat}/K_m)^{obsd}/[H^+]$, as shown in Figure 5, we determined apparent kinetic pK_a values of 6.2 and 6.3, respectively, for the titratable group in DTA-wt.

Discussion

On the basis of early kinetic analysis of the ADP-ribosylation of EF-2 by DTA (Kandel et al., 1974; Collier et al., 1974; Chung & Collier, 1977), it was proposed that the

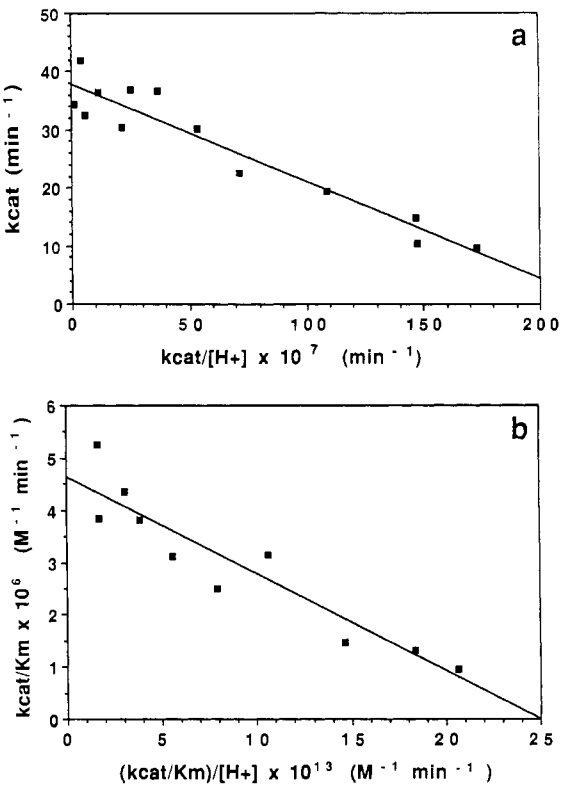

FIGURE 5: (a) k_{cat} vs $k_{cat}/[H^+]$ and (b) k_{cat}/K_m vs $(k_{cat}/K_m)/[H^+]$ for ADP-ribosylation of EF-2 by DTA-wt. The kinetic data were obtained at varying pH values as described in the text. The respective apparent kinetic pK_a values, determined from the slopes of the curves, were (a) 6.2 and (b) 6.3.

reaction proceeds by an ordered sequential mechanism, the sequence of binding of substrates being NAD followed by EF-2. No covalent enzyme–substrate intermediates have been found (Kandel et al., 1974; Chung & Collier, 1977; Collier, 1982), and the toxin does not appear to catalyze exchange of the nicotinamide moiety (Collier, 1982). Identification of Glu-148 as a putative active-site residue of DTA came from experiments in which this residue was shown to be efficiently and specifically photolabeled in the presence of nicotinamide-radiolabeled NAD (Carroll & Collier, 1984; Carroll et al., 1985a,b). The photoproduct at position 148 was found to contain the nicotinamide ring linked via its C_6 to the decarboxylated γ-methylene group of the glutamic acid residue (Carroll et al., 1985a,b). This structure suggested that the member atoms of the new C–C bond formed in the photoreaction are in close proximity in the DTA–NAD complex, which is formed in the initial step of ADP-ribosylation of EF-2. This would place the side-chain carboxyl group of Glu-148 within a short radius of the nicotinamide C_6 and possibly in contact with the nicotinamide–glycosyl linkage disrupted in either of the ADP-ribosyl transfer and NAD hydrolysis reactions catalyzed by DTA. Thus, the carboxyl group of Glu-148 might in fact participate directly in catalysis. As a consequence, we were led to pursue further studies on the possible role of Glu-148 in catalysis by using site-directed mutagenesis to replace this residue.

Tweten et al. (1985) substituted aspartic acid for Glu-148 in the cloned F2 fragment of diphtheria toxin in *E. coli* and estimated the ADP-ribosyltransferase activity of the derived mutant fragment A in crude extracts to be less than 0.6% that of wild-type DTA. The mutation produced no change in trypsin sensitivity, and there was little reduction in affinity for NAD. Barbieri and Collier (1987) later generated a serine substitution at position 148 and estimated, again in crude

extracts of *E. coli*, that ADP-ribosylation of EF-2 proceeded at a rate less than 0.3% that of wild-type DTA. In the current work we have prepared purified mutant forms of DTA containing either of these mutations or a third mutation, E148Q, and have presented more detailed studies on their catalytic properties.

The results indicate that even the most conservative substitutions at position 148 cause drastic reductions in ADP-ribosyltransferase activity, while producing only minimal changes in affinity for NAD and EF-2 substrates. Replacement of Glu-148 with either aspartic acid, glutamine, or serine diminished activity by ca. 100-, 250-, or 300-fold, respectively, while causing little change in K_m or K_d for NAD or K_m for EF-2. The magnitudes of reduction in ADP-ribosyltransferase activity for the mutant toxins E148D and E148S were consistent with the estimated activities reported earlier for these mutants in crude *E. coli* extracts (Tweten et al., 1985; Barbieri & Collier, 1987), which indicates little inactivation during the purification process. In agreement with earlier results (Tweten et al., 1985), the relatively conservative amino acid changes at position 148 caused no increase in sensitivity to trypsin, implying that these substitutions produced little or no alteration in the overall protein structure.

The retention of substrate affinities further showed that the major effects of the mutations were confined to k_{cat}, supporting the supposition that Glu-148 plays an important role in enzymic catalysis. Thus, even relatively conservative changes such as withdrawal of the carboxyl group at position 148 by one methylene unit, as in the aspartate mutant, or replacement of the carboxyl group by an uncharged amide, as in the glutamine mutant, virtually abolish ADP-ribosyltransferase activity. This implies that the precise spatial position and charge of the carboxyl side chain are crucial for catalysis and supports the notion that this group may participate directly in catalysis. Failure of the isosteric glutamine to function effectively in place of glutamic acid suggests that it is not the hydrogen-bond-forming capability of the carboxyl group, but rather its acidic function, which is important for catalysis. The somewhat greater activity of the aspartic acid mutant, which withdraws the functional group by one methylene while maintaining its acidic properties, over the glutamine mutant supports this proposal.

There are several conceivable ways in which the carboxyl group might function in catalyzing the ADP-ribosylation of EF-2: (i) by initially interacting with the quaternary nitrogen center and then acting as an acceptor for the proton liberated as a product of the reaction, (ii) by serving as a general base to deprotonate the attacking diphthamide residue in an S_N2-type displacement reaction, (iii) by providing electrostatic stabilization of a cationic transition state intermediate in an S_N1-like mechanism, or (iv) by maintaining important hydrogen-bonding interaction(s) or conformational structure of the active site necessary for catalysis to occur. In order to determine which, if any, of these catalytic functions the glutamic acid may serve, we examined the pH dependence of k_{cat} and k_{cat}/K_m of the ADP-ribosyltransferase reaction of DTA for the wild-type protein and two of the active-site mutants, DTA-E148Q and DTA-E148S (Figure 4).

For a reaction in which all intermediates are in protonic equilibrium and the decomposition of enzyme–substrate complex is rate-limiting, a plot of $(k_{cat}/K_m)^{obsd}$ vs pH yields the apparent pK value for free enzyme and/or substrate, and a plot of $(k_{cat})^{obsd}$ vs pH provides the apparent pK value of the kinetically most significant enzyme–substrate complex—that whose decomposition to product is rate-limiting (Knowles, 1976; Cleland, 1977; Dixon & Webb, 1980; Fersht, 1985). The curves in Figure 4 for DTA-wt reveal the presence of a titratable group that is dramatically affected by substitution of glutamine or serine for Glu-148. Furthermore, this group must be protonated for ADP-ribosylation to occur, since the reaction rate declined with increasing pH. By using plots analagous to the well-known Eadie–Hofstee plots, we extracted apparent kinetic pK_a values of 6.2 and 6.3 for k_{cat} and $k_{cat}/K_{m(NAD)}$, respectively. As the same titration appears in both the k_{cat} and k_{cat}/K_m profiles, it probably corresponds to a group that titrates in both the DTA–NAD–EF-2 and DTA–NAD complexes, thus diminishing the possibility that we may be observing the ionization of a group on the substrate EF-2.

Although it is conceivable that the observed pK_a of 6.2–6.3 may correspond to the carboxyl group of Glu-148 (Fersht, 1985), this is above the normal range of pK_a values for the side-chain carboxyl group of glutamic acid in proteins. A more complex interpretation of these results must therefore be considered. From sequence comparisons, it is known that the single histidine in DTA (His-21) is a highly conserved residue found in all ADP-ribosylating toxins whose sequences are known, including DT, *P. aeruginosa* exotoxin A, cholera toxin, pertussis toxins, and others (Rappuoli & Pizza, 1990). From the X-ray crystal structure of *P. aeruginosa* exotoxin A (Allured et al., 1986), it may be deduced that the conserved histidine corresponding to His-21 of DT lies within the active-site pocket (Carroll & Collier, 1988). Additionally, it has been shown by Papini et al. (E. Papini, G. Schiavo, R. Rappuoli, and C. Montecucco, personal communication, 1990) that chemical modification of His-21 results in complete loss of NAD binding and enzymatic activity. Papini and co-workers have also obtained independent evidence that His-21 titrates with a pK_a value of 6.3, from examination of the pH dependence of both NAD binding and diethyl pyrocarbonate modification of His-21. We therefore feel that the observed kinetic titration probably represents the ionization of the His-21 side-chain imidazole and that the presence of Glu-148 strongly affects this titration.

The role of the carboxyl group of Glu-148 is an intriguing question. Although more complex interpretations are possible, our results suggest that a combination of both models ii and iv proposed above for the function of the carboxyl group in catalysis may contribute to the reaction mechanism. The glutamic acid may be important for maintaining a particular active-site conformation necessary for catalysis to occur, such as confining the position of the imidazole ring of His-21. The absence of a pK_a of 6.2–6.3 in the pH profiles of the E148Q and E148S mutants suggests the carboxyl group may function primarily by altering the pK_a of the histidine. Similar acid–base interaction between two or more active-site residues has been proposed for the serine and aspartyl proteases (Fersht, 1985). If this is the case, their ionizations would give a pH–activity profile similar to that obtained, which depends upon the acidic form of an imidazole group with a pK_a > 6 and the basic form of a carboxyl group with a pK_a < 6. As a result of this acid–base interaction, the nucleophilicity of the incoming diphthamide may be increased.

Since it is unlikely that NAD is bound differently for ADP-ribosylation than for NAD-glycohydrolysis, the results obtained for the NAD-glycohydrolase activity suggest that the catalytic mechanism of this reaction may be different from that of the ADP-ribosylation reaction. The substitutions at position 148 affected NAD-glycohydrolase activity to a much lesser extent than ADP-ribosyltransferase activity, implying that the carboxyl group may not be important for hydrolysis

of the glycosyl–nicotinamide linkage. The absence of a significant decrease in NAD-glycohydrolase activity of the mutants further supports the catalytic importance of glutamic acid in the ADP-ribosylation reaction and diminishes the likelihood that the role of the carboxyl group is to provide electrostatic stabilization of a cationic transition state intermediate, as proposed above in model iii. Two of the mutants, E148D and E148Q, even displayed a small but reproducible increase in NAD-glycohydrolytic activity. Considering the large difference in the k_{cat} for these two reactions, NAD-glycohydrolase activity may represent a reaction caused by distortion of the NAD molecule, which might occur upon binding to DTA, thereby facilitating the hydrolytic process. There is no evidence that the weak NAD-glycohydrolase activity is physiologically significant.

The ability of the E148D mutant to be photolabeled is consistent with the proposed positioning of Glu-148 within the active site and in close proximity to the nicotinamide ring of enzyme-bound NAD. Displacing the carboxyl group (E148D) by one methylene unit reduces the rate of photolabeling 8-fold, indicating that photoadduct formation is sensitive to the presence and positioning of the carboxyl group at position 148. Removal of the carboxyl group at position 148 in DTA (E148Q or E148S) reduces the rate of photolabeling to undetectable levels.

We have not studied the photochemical reaction mechanism in detail, but we believe that a mechanism involving radical coupling, followed by decarboxylation and oxidation, may be occurring. The primary excitation event is most likely photon absorption by the nicotinamide ring. Photoinduced decarboxylation of the carboxy-terminal amino acid of peptides has been observed in the presence of anthraquinone antitumor agents (Carmichael & Riesz, 1985). Photoexcitation of complexes of oxidized lactate oxidase and alkylcarboxylic acids has been shown to induce decarboxylation and adduct formation of bound acid with the flavin cofactor (Ghisla et al., 1979). Chemical precedence for the observed photoreaction can be found in the well-known photochemical alkylation of imines in aromatic nitrogen heterocycles, including purine, pyrimidine, acridine, pyridine, benzimidazole, quinoline, and similar compounds, by alkylcarboxylic acids and acidified alcohols (Nozaki et al., 1967; Stermitz et al., 1968; Chapman, 1969; Linschitz & Connolly, 1968; Ochiai & Morita, 1967). The reaction with carboxylic acids yields products from radical recombination, followed by decarboxylation and oxidation. With alcohols, the intermediates formed by combination of the initially produced radicals have to undergo acid catalysis to give the final products. The lack of photolabeling observed for the E148Q and E148S mutants is consistent with the requirement of an acidic functionality for photoadduct formation.

Diphtheria toxin is one of two well-characterized ADP-ribosyltransferase enzymes for which an active-site glutamic acid, identified by photolabeling with NAD, has been shown to play an important role in catalysis. In *P. aeruginosa* exotoxin A, Douglas and Collier (1987) have demonstrated a >1000-fold decrease in catalytic activity of this proenzyme upon substitution of the photolabeled Glu-553 by aspartic acid. The structural and primary amino acid sequence differences between DT and ETA only highlight the functional similarities of these enzymes. Both proteins catalyze identical reactions with comparable enzymatic and kinetic parameters, both are secreted in cytotoxic but catalytically inactive proenzyme forms, and both require an active-site glutamic acid residue for NAD:EF-2 ADP-ribosylation. Recently, it has been demonstrated (Barbieri et al., 1989; Cockle, 1989; Cieplak et al., 1990) that a cloned derivative of the catalytic S-1 subunit of pertussis toxin also undergoes a similar photochemical reaction in which Glu-129 is specifically photolabeled. When DT Glu-148 was aligned with ETA Glu-553, a local region of considerable sequence homology was observed (Brandhuber et al., 1988; Gill, 1988; Zhao & London, 1988; Carroll & Collier, 1988; Collier, 1989). However, no similar sequence homology was found between pertussis S-1 subunit and DTA or ETA (Barbieri et al., 1989), and although S-1 shares some sequence similarity with cholera toxin, the residue in cholera toxin corresponding to Glu-129 in S-1 is not a glutamic acid but instead a tryptophan (Trp-127) (Barbieri et al., 1989). On the other hand, as mentioned above, a consistent feature among all ADP-ribosylating toxins appears to be the presence of an active-site histidine residue. If the photolabeled glutamic acids of the three toxins do indeed function in the same way and interact with the conserved histidines, then the topology of the active sites might be such that another amino acid carboxyl group is in close proximity and can serve an analogous role in catalysis for the other toxins as well.

Acknowledgments

We thank Dr. Joel G. Belasco for a critical reading of this manuscript and helpful discussion and Drs. Cesare Montecucco, Rino Rappuoli, and Emanuele Papini for valuable input regarding the relevance of His-21.

Registry No. L-Glu, 56-86-0; NAD:EF-2 ADP-ribosyltransferase, 52933-21-8; NAD-glycohydrolase, 9032-92-2.

References

Allured, V. S., Collier, R. J., Carroll, S. F., & McKay, D. B. (1986) *Proc. Natl. Acad. Sci. U.S.A. 83*, 1320–1324.

Barbieri, J. T., & Collier, R. J. (1987) *Infect. Immun. 55*, 1647–1651.

Barbieri, J. T., Mende-Mueller, L. M., Rappuoli, R., & Collier, R. J. (1989) *Infect. Immun. 57*, 3549–3554.

Brandhuber, B. J., Allured, V. S., Falbel, T. G., & McKay, D. B. (1988) *Proteins: Struct., Funct., Genet. 3*, 146–154.

Carmichael, A. J., & Riesz, P. (1985) *Arch. Biochem. Biophys. 237*, 433–444.

Carroll, S. F., & Collier, R. J. (1984) *Proc. Natl. Acad. Sci. U.S.A. 81*, 3307–3311.

Carroll, S. F., & Collier, R. J. (1987) *J. Biol. Chem. 262*, 8707–8711.

Carroll, S. F., & Collier, R. J. (1988) *Mol. Microbiol. 2*, 293–296.

Carroll, S. F., McCloskey, J. A., Crain, P. F., Oppenheimer, N. J., Marschner, T. M., & Collier, R. J. (1985a) *Proc. Natl. Acad. Sci. U.S.A. 82*, 7237–7241.

Carroll, S. F., Oppenheimer, N. J., Marschner, T. M., McCloskey, J. A., Crain, P. F., & Collier, R. J. (1985b) in *ADP-Ribosylation of Proteins* (Althaus, F. R., Hilz, H., & Shall, S., Eds.) pp 544–550, Springer-Verlag, New York.

Chapman, O. L. (1969) *Organic Photochemistry*, Marcel Dekker, New York.

Chung, D. W., & Collier, R. J. (1977) *Biochim. Biophys. Acta 483*, 248–257.

Cieplak, W., Locht, C., Mar, V. L., Burnette, W. N., & Keith, J. M. (1990) *Biochem. J. 268*, 547–551.

Cleland, W. W. (1977) *Adv. Enzymol. Relat. Areas Mol. Biol. 45*, 273–388.

Cockle, S. A. (1989) *FEBS Lett. 249*, 329–332.

Collier, R. J. (1982) in *ADP-Ribosylation Reactions* (Hayaishi, O., & Ueda, K., Eds.) pp 575–592, Academic Press, New York.

Collier, R. J. (1986) in *Protein–Carbohydrate Interactions in Biological Systems* (Lark, D. L., Ed.) pp 399–405, Academic Press, New York.

Collier, R. J. (1989) in *ADP-Ribose Transfer Reactions: Mechanisms and Biological Significance* (Jacobson, M. K., & Jacobson, E. L., Eds.) pp 458–462, Springer-Verlag, New York.

Collier, R. J., & Mekalanos, J. J. (1980) in *Multifunctional Proteins* (Bisswanger, H., & Schmincke-Ott, E., Eds.) pp 261–291, John Wiley & Sons, New York.

Collier, R. J., DeLange, R. J., Drazin, R., Kandel, J., & Chung, D. W. (1974) in *Poly(ADP-Ribose), An International Symposium* (Harris, M., Ed.) pp 287–304, DHEW Publication No. (NIH) 74-477, U.S. Government Printing Office, Washington, DC.

de Boer, H. A., Comstock, L. J. & Vasser, M. (1983) *Proc. Natl. Acad. Sci. U.S.A. 80*, 21–25.

Dixon, M., & Webb, E. L. (1980) *Enzymes*, Academic Press, New York.

Douglas, C. D., & Collier, R. J. (1987) *J. Bacteriol. 169*, 4967–4971.

Douglas, C. M., Guidi-Rontani, C., & Collier, R. J. (1987) *J. Bacteriol. 169*, 4962–4966.

Fersht, A. (1985) *Enzyme Structure and Mechanism*, W. H. Freeman, New York.

Fischetti, V. A., Jarymowycz, M., Jones, K. F., & Scott, J. R. (1986) *J. Exp. Med. 164*, 971–980.

Ghisla, S., Massey, V., & Choong, Y. S. (1979) *J. Biol. Chem. 254*, 10662–10669.

Gill, D. M. (1988) in *Bacterial Protein Toxins, Third European Workshop* (Fehrenbach, F. E., Falmagne, P., Boebel, W., Jeljaszewicz, J., Jurgens, D., & Rappuoli, R., Eds.) pp 315–323, Gustav Fischer, New York.

Jacobson, M. K., & Jacobson, E. L. (1989) *ADP-Ribose Transfer Reactions. Mechanisms and Biological Significance*, Springer-Verlag, New York.

Kandel, J., Collier, R. J., & Chung, D. W. (1974) *J. Biol. Chem. 249*, 2088–2097.

Knowles, J. R. (1976) *CRC Crit. Rev. Biochem. 4*, 165–173.

Leong, D., Coleman, K. D., & Murphy, J. R. (1983a) *J. Biol. Chem. 258*, 15016–15020.

Leong, D., Coleman, K. D., & Murphy, J. R. (1983b) *Science 220*, 515–517.

Linschitz, H., & Connolly, J. S. (1968) *J. Am. Chem. Soc. 90*, 2979–2980.

Lukac, M., & Collier, R. J. (1988) *J. Biol. Chem. 263*, 6146–6149.

Lukac, M., Pier, G. B., & Collier, R. J. (1988) *Infect. Immun. 56*, 3095–3098.

Maniatis, T., Fritsch, E. F., & Sambrook, J. (1982) *Molecular Cloning: A Laboratory Manual*, Cold Spring Harbor Laboratory, Cold Spring Harbor, NY.

Nozaki, H., Kato, M., Noyori, R., & Kawanisi, M. (1967) *Tetrahedron Lett. 43*, 4259–4260.

Ochiai, M., & Morita, K. (1967) *Tetrahedron Lett. 43*, 2349–2351.

Papini, E., Schiavo, G., Sandona, D., Rappuoli, R. & Montecucco, C. (1989) *J. Biol. Chem. 264*, 12385–12388.

Rappuoli, R., & Pizza, M. (1990) in *Structure, Regulation and Activity of Bacterial Toxins* (Alouf, J., & Freer, J., Eds.) Academic Press, NY (in press).

Sanger, F., Nicklen, S., & Coulson, A. R. (1977) *Proc. Natl. Acad. Sci. U.S.A. 74*, 5463–5467.

Stermitz, F. R., Wei, C. C., & Huang, W. H. (1968) *Chem. Commun.* 482–483.

Taylor, J. W., Ott, J., & Eckstein, F. (1985a) *Nucleic Acids Res. 13*, 8764–8785.

Taylor, J. W., Schmidt, W., Cosstick, R., Okruszek, A., & Eckstein, F. (1985b) *Nucleic Acids Res. 13*, 8749–8764.

Tweten, R. K., & Collier, R. J. (1983) *J. Bacteriol. 156*, 680–685.

Tweten, R. K., Barbieri, J. T., & Collier, R. J. (1985) *J. Biol. Chem. 260*, 10392–10394.

Zhao, J.-M., & London, E. (1988) *Biochemistry 27*, 3398–3403.

Zoller, M. J., & Smith, M. (1983) *Methods Enzymol. 100*, 468–500.